Search for Charged Massive Long-Lived Particles

V. M. Abazov,[34] B. Abbott,[72] B. S. Acharya,[28] M. Adams,[48] T. Adams,[46] G. D. Alexeev,[34] J. Alimena,[74] G. Alkhazov,[38] A. Alton,[60,†] G. Alverson,[59] G. A. Alves,[2] M. Aoki,[47] A. Askew,[46] B. Åsman,[40] S. Atkins,[57] O. Atramentov,[64] K. Augsten,[9] C. Avila,[7] J. BackusMayes,[79] F. Badaud,[12] L. Bagby,[47] B. Baldin,[47] D. V. Bandurin,[46] S. Banerjee,[28] E. Barberis,[59] P. Baringer,[55] J. Barreto,[3] J. F. Bartlett,[47] U. Bassler,[17] V. Bazterra,[48] A. Bean,[55] M. Begalli,[3] C. Belanger-Champagne,[40] L. Bellantoni,[47] S. B. Beri,[26] G. Bernardi,[16] R. Bernhard,[21] I. Bertram,[41] M. Besançon,[17] R. Beuselinck,[42] V. A. Bezzubov,[37] P. C. Bhat,[47] V. Bhatnagar,[26] G. Blazey,[49] S. Blessing,[46] K. Bloom,[63] A. Boehnlein,[47] D. Boline,[69] E. E. Boos,[36] G. Borissov,[41] T. Bose,[58] A. Brandt,[75] O. Brandt,[22] R. Brock,[61] G. Brooijmans,[67] A. Bross,[47] D. Brown,[16] J. Brown,[16] X. B. Bu,[47] M. Buehler,[47] V. Buescher,[23] V. Bunichev,[36] S. Burdin,[41,‡] T. H. Burnett,[79] C. P. Buszello,[40] B. Calpas,[14] E. Camacho-Pérez,[31] M. A. Carrasco-Lizarraga,[55] B. C. K. Casey,[47] H. Castilla-Valdez,[31] S. Chakrabarti,[69] D. Chakraborty,[49] K. M. Chan,[53] A. Chandra,[77] E. Chapon,[17] G. Chen,[55] S. Chevalier-Théry,[17] D. K. Cho,[74] S. W. Cho,[30] S. Choi,[30] B. Choudhary,[27] S. Cihangir,[47] D. Claes,[63] J. Clutter,[55] M. Cooke,[47] W. E. Cooper,[47] M. Corcoran,[77] F. Couderc,[17] M.-C. Cousinou,[14] A. Croc,[17] D. Cutts,[74] A. Das,[44] G. Davies,[42] K. De,[75] S. J. de Jong,[33] E. De La Cruz-Burelo,[31] F. Déliot,[17] R. Demina,[68] D. Denisov,[47] S. P. Denisov,[37] S. Desai,[47] C. Deterre,[17] K. DeVaughan,[63] H. T. Diehl,[47] M. Diesburg,[47] P. F. Ding,[43] A. Dominguez,[63] T. Dorland,[79] A. Dubey,[27] L. V. Dudko,[36] D. Duggan,[64] A. Duperrin,[14] S. Dutt,[26] A. Dyshkant,[49] M. Eads,[63] D. Edmunds,[61] J. Ellison,[45] V. D. Elvira,[47] Y. Enari,[16] H. Evans,[51] A. Evdokimov,[70] V. N. Evdokimov,[37] G. Facini,[59] T. Ferbel,[68] F. Fiedler,[23] F. Filthaut,[33] W. Fisher,[61] H. E. Fisk,[47] M. Fortner,[49] H. Fox,[41] S. Fuess,[47] A. Garcia-Bellido,[68] G. A García-Guerra,[31,§] V. Gavrilov,[35] P. Gay,[12] W. Geng,[14,61] D. Gerbaudo,[65] C. E. Gerber,[48] Y. Gershtein,[64] G. Ginther,[47,68] G. Golovanov,[34] A. Goussiou,[79] P. D. Grannis,[69] S. Greder,[18] H. Greenlee,[47] Z. D. Greenwood,[57] E. M. Gregores,[4] G. Grenier,[19] Ph. Gris,[12] J.-F. Grivaz,[15] A. Grohsjean,[17] S. Grünendahl,[47] M. W. Grünewald,[29] T. Guillemin,[15] G. Gutierrez,[47] P. Gutierrez,[72] A. Haas,[67,‖] S. Hagopian,[46] J. Haley,[59] L. Han,[6] K. Harder,[43] A. Harel,[68] J. M. Hauptman,[54] J. Hays,[42] T. Head,[43] T. Hebbeker,[20] D. Hedin,[49] H. Hegab,[73] A. P. Heinson,[45] U. Heintz,[74] C. Hensel,[22] I. Heredia-De La Cruz,[31] K. Herner,[60] G. Hesketh,[43,¶] M. D. Hildreth,[53] R. Hirosky,[78] T. Hoang,[46] J. D. Hobbs,[69] B. Hoeneisen,[11] M. Hohlfeld,[23] Z. Hubacek,[9,17] V. Hynek,[9] I. Iashvili,[66] Y. Ilchenko,[76] R. Illingworth,[47] A. S. Ito,[47] S. Jabeen,[74] M. Jaffré,[15] D. Jamin,[14] A. Jayasinghe,[72] R. Jesik,[42] K. Johns,[44] M. Johnson,[47] A. Jonckheere,[47] P. Jonsson,[42] J. Joshi,[26] A. W. Jung,[47] A. Juste,[39] K. Kaadze,[56] E. Kajfasz,[14] D. Karmanov,[36] P. A. Kasper,[47] I. Katsanos,[63] R. Kehoe,[76] S. Kermiche,[14] N. Khalatyan,[47] A. Khanov,[73] A. Kharchilava,[66] Y. N. Kharzheev,[34] J. M. Kohli,[26] A. V. Kozelov,[37] J. Kraus,[61] S. Kulikov,[37] A. Kumar,[66] A. Kupco,[10] T. Kurča,[19] V. A. Kuzmin,[36] J. Kvita,[8] S. Lammers,[51] G. Landsberg,[74] P. Lebrun,[19] H. S. Lee,[30] S. W. Lee,[54] W. M. Lee,[47] J. Lellouch,[16] L. Li,[45] Q. Z. Li,[47] S. M. Lietti,[5] J. K. Lim,[30] D. Lincoln,[47] J. Linnemann,[61] V. V. Lipaev,[37] R. Lipton,[47] Y. Liu,[6] A. Lobodenko,[38] M. Lokajicek,[10] R. Lopes de Sa,[69] H. J. Lubatti,[79] R. Luna-Garcia,[31,**] A. L. Lyon,[47] A. K. A. Maciel,[2] D. Mackin,[77] R. Madar,[17] R. Magaña-Villalba,[31] S. Malik,[63] V. L. Malyshev,[34] Y. Maravin,[56] J. Martínez-Ortega,[31] R. McCarthy,[69] C. L. McGivern,[55] M. M. Meijer,[33] A. Melnitchouk,[62] D. Menezes,[49] P. G. Mercadante,[4] M. Merkin,[36] A. Meyer,[20] J. Meyer,[22] F. Miconi,[18] N. K. Mondal,[28] G. S. Muanza,[14] M. Mulhearn,[78] E. Nagy,[14] M. Naimuddin,[27] M. Narain,[74] R. Nayyar,[27] H. A. Neal,[60] J. P. Negret,[7] P. Neustroev,[38] S. F. Novaes,[5] T. Nunnemann,[24] G. Obrant,[38,*] J. Orduna,[77] N. Osman,[14] J. Osta,[53] G. J. Otero y Garzón,[1] M. Padilla,[45] A. Pal,[75] N. Parashar,[52] V. Parihar,[74] S. K. Park,[30] R. Partridge,[74,‖] N. Parua,[51] A. Patwa,[70] B. Penning,[47] M. Perfilov,[36] Y. Peters,[43] K. Petridis,[43] G. Petrillo,[68] P. Pétroff,[15] R. Piegaia,[1] M.-A. Pleier,[70] P. L. M. Podesta-Lerma,[31,††] V. M. Podstavkov,[47] P. Polozov,[35] A. V. Popov,[37] M. Prewitt,[77] D. Price,[51] N. Prokopenko,[37] J. Qian,[60] A. Quadt,[22] B. Quinn,[62] M. S. Rangel,[2] K. Ranjan,[27] P. N. Ratoff,[41] I. Razumov,[37] P. Renkel,[76] M. Rijssenbeek,[69] I. Ripp-Baudot,[18] F. Rizatdinova,[73] M. Rominsky,[47] A. Ross,[41] C. Royon,[17] P. Rubinov,[47] R. Ruchti,[53] G. Safronov,[35] G. Sajot,[13] P. Salcido,[49] A. Sánchez-Hernández,[31] M. P. Sanders,[24] B. Sanghi,[47] A. S. Santos,[5] G. Savage,[47] L. Sawyer,[57] T. Scanlon,[42] R. D. Schamberger,[69] Y. Scheglov,[38] H. Schellman,[50] T. Schliephake,[25] S. Schlobohm,[79] C. Schwanenberger,[43] R. Schwienhorst,[61] J. Sekaric,[55] H. Severini,[72] E. Shabalina,[22] V. Shary,[17] A. A. Shchukin,[37] R. K. Shivpuri,[27] V. Simak,[9] V. Sirotenko,[47] P. Skubic,[72] P. Slattery,[68] D. Smirnov,[53] K. J. Smith,[66] G. R. Snow,[63] J. Snow,[71] S. Snyder,[70] S. Söldner-Rembold,[43] L. Sonnenschein,[20] K. Soustruznik,[8] J. Stark,[13] V. Stolin,[35] D. A. Stoyanova,[37] M. Strauss,[72] D. Strom,[48] L. Stutte,[47] L. Suter,[43] P. Svoisky,[72] M. Takahashi,[43] A. Tanasijczuk,[1] M. Titov,[17] V. V. Tokmenin,[34] Y.-T. Tsai,[68] K. Tschann-Grimm,[69] D. Tsybychev,[69] B. Tuchming,[17] C. Tully,[65] L. Uvarov,[38] S. Uvarov,[38] S. Uzunyan,[49] R. Van Kooten,[51] W. M. van Leeuwen,[32] N. Varelas,[48] E. W. Varnes,[44] I. A. Vasilyev,[37] P. Verdier,[19] L. S. Vertogradov,[34] M. Verzocchi,[47] M. Vesterinen,[43] D. Vilanova,[17] P. Vokac,[9] H. D. Wahl,[46]

M. H. L. S. Wang,[47] J. Warchol,[53] G. Watts,[79] M. Wayne,[53] M. Weber,[47,‡‡] L. Welty-Rieger,[50] A. White,[75] D. Wicke,[25] M. R. J. Williams,[41] G. W. Wilson,[55] M. Wobisch,[57] D. R. Wood,[59] T. R. Wyatt,[43] Y. Xie,[47] R. Yamada,[47] W.-C. Yang,[43] T. Yasuda,[47] Y. A. Yatsunenko,[34] Z. Ye,[47] H. Yin,[47] K. Yip,[70] S. W. Youn,[47] J. Yu,[75] T. Zhao,[79] B. Zhou,[60] J. Zhu,[60] M. Zielinski,[68] D. Zieminska,[51] and L. Zivkovic[74]

(D0 Collaboration)

[1]*Universidad de Buenos Aires, Buenos Aires, Argentina*
[2]*LAFEX, Centro Brasileiro de Pesquisas Físicas, Rio de Janeiro, Brazil*
[3]*Universidade do Estado do Rio de Janeiro, Rio de Janeiro, Brazil*
[4]*Universidade Federal do ABC, Santo André, Brazil*
[5]*Instituto de Física Teórica, Universidade Estadual Paulista, São Paulo, Brazil*
[6]*University of Science and Technology of China, Hefei, People's Republic of China*
[7]*Universidad de los Andes, Bogotá, Colombia*
[8]*Charles University, Faculty of Mathematics and Physics, Center for Particle Physics, Prague, Czech Republic*
[9]*Czech Technical University in Prague, Prague, Czech Republic*
[10]*Center for Particle Physics, Institute of Physics, Academy of Sciences of the Czech Republic, Prague, Czech Republic*
[11]*Universidad San Francisco de Quito, Quito, Ecuador*
[12]*LPC, Université Blaise Pascal, CNRS/IN2P3, Clermont, France*
[13]*LPSC, Université Joseph Fourier Grenoble 1, CNRS/IN2P3, Institut National Polytechnique de Grenoble, Grenoble, France*
[14]*CPPM, Aix-Marseille Université, CNRS/IN2P3, Marseille, France*
[15]*LAL, Université Paris-Sud, CNRS/IN2P3, Orsay, France*
[16]*LPNHE, Universités Paris VI and VII, CNRS/IN2P3, Paris, France*
[17]*CEA, Irfu, SPP, Saclay, France*
[18]*IPHC, Université de Strasbourg, CNRS/IN2P3, Strasbourg, France*
[19]*IPNL, Université Lyon 1, CNRS/IN2P3, Villeurbanne, France and Université de Lyon, Lyon, France*
[20]*III. Physikalisches Institut A, RWTH Aachen University, Aachen, Germany*
[21]*Physikalisches Institut, Universität Freiburg, Freiburg, Germany*
[22]*II. Physikalisches Institut, Georg-August-Universität Göttingen, Göttingen, Germany*
[23]*Institut für Physik, Universität Mainz, Mainz, Germany*
[24]*Ludwig-Maximilians-Universität München, München, Germany*
[25]*Fachbereich Physik, Bergische Universität Wuppertal, Wuppertal, Germany*
[26]*Panjab University, Chandigarh, India*
[27]*Delhi University, Delhi, India*
[28]*Tata Institute of Fundamental Research, Mumbai, India*
[29]*University College Dublin, Dublin, Ireland*
[30]*Korea Detector Laboratory, Korea University, Seoul, Korea*
[31]*CINVESTAV, Mexico City, Mexico*
[32]*Nikhef, Science Park, Amsterdam, The Netherlands*
[33]*Radboud University Nijmegen, Nijmegen, The Netherlands and Nikhef, Science Park, Amsterdam, The Netherlands*
[34]*Joint Institute for Nuclear Research, Dubna, Russia*
[35]*Institute for Theoretical and Experimental Physics, Moscow, Russia*
[36]*Moscow State University, Moscow, Russia*
[37]*Institute for High Energy Physics, Protvino, Russia*
[38]*Petersburg Nuclear Physics Institute, St. Petersburg, Russia*
[39]*Institució Catalana de Recerca i Estudis Avançats (ICREA) and Institut de Física d'Altes Energies (IFAE), Barcelona, Spain*
[40]*Stockholm University, Stockholm and Uppsala University, Uppsala, Sweden*
[41]*Lancaster University, Lancaster LA1 4YB, United Kingdom*
[42]*Imperial College London, London SW7 2AZ, United Kingdom*
[43]*The University of Manchester, Manchester M13 9PL, United Kingdom*
[44]*University of Arizona, Tucson, Arizona 85721, USA*
[45]*University of California Riverside, Riverside, California 92521, USA*
[46]*Florida State University, Tallahassee, Florida 32306, USA*
[47]*Fermi National Accelerator Laboratory, Batavia, Illinois 60510, USA*
[48]*University of Illinois at Chicago, Chicago, Illinois 60607, USA*
[49]*Northern Illinois University, DeKalb, Illinois 60115, USA*
[50]*Northwestern University, Evanston, Illinois 60208, USA*
[51]*Indiana University, Bloomington, Indiana 47405, USA*
[52]*Purdue University Calumet, Hammond, Indiana 46323, USA*

[53]University of Notre Dame, Notre Dame, Indiana 46556, USA
[54]Iowa State University, Ames, Iowa 50011, USA
[55]University of Kansas, Lawrence, Kansas 66045, USA
[56]Kansas State University, Manhattan, Kansas 66506, USA
[57]Louisiana Tech University, Ruston, Louisiana 71272, USA
[58]Boston University, Boston, Massachusetts 02215, USA
[59]Northeastern University, Boston, Massachusetts 02115, USA
[60]University of Michigan, Ann Arbor, Michigan 48109, USA
[61]Michigan State University, East Lansing, Michigan 48824, USA
[62]University of Mississippi, University, Mississippi 38677, USA
[63]University of Nebraska, Lincoln, Nebraska 68588, USA
[64]Rutgers University, Piscataway, New Jersey 08855, USA
[65]Princeton University, Princeton, New Jersey 08544, USA
[66]State University of New York, Buffalo, New York 14260, USA
[67]Columbia University, New York, New York 10027, USA
[68]University of Rochester, Rochester, New York 14627, USA
[69]State University of New York, Stony Brook, New York 11794, USA
[70]Brookhaven National Laboratory, Upton, New York 11973, USA
[71]Langston University, Langston, Oklahoma 73050, USA
[72]University of Oklahoma, Norman, Oklahoma 73019, USA
[73]Oklahoma State University, Stillwater, Oklahoma 74078, USA
[74]Brown University, Providence, Rhode Island 02912, USA
[75]University of Texas, Arlington, Texas 76019, USA
[76]Southern Methodist University, Dallas, Texas 75275, USA
[77]Rice University, Houston, Texas 77005, USA
[78]University of Virginia, Charlottesville, Virginia 22901, USA
[79]University of Washington, Seattle, Washington 98195, USA
(Received 17 October 2011; published 21 March 2012)

We report on a search for charged massive long-lived particles (CMLLPs), based on 5.2 fb^{-1} of integrated luminosity collected with the D0 detector at the Fermilab Tevatron $p\bar{p}$ collider. We search for events in which one or more particles are reconstructed as muons but have speed and ionization energy loss (dE/dx) inconsistent with muons produced in beam collisions. CMLLPs are predicted in several theories of physics beyond the standard model. We exclude pair-produced long-lived gauginolike charginos below 267 GeV and Higgsino-like charginos below 217 GeV at 95% C.L., as well as long-lived scalar top quarks with mass below 285 GeV.

DOI: 10.1103/PhysRevLett.108.121802 PACS numbers: 13.85.Rm, 14.80.Ly

We report on a search for massive particles that are electrically charged and have a lifetime long enough to escape the D0 detector before decaying. Charged massive long-lived particles are not present in the standard model (SM) nor are their distinguishing characteristics (slow speed, high dE/dx) relevant for most high energy physics studies. Although the distinctive signature in itself provides sufficient motivation for a search, some recent extensions to the SM suggest that charged massive long-lived particles (CMLLPs) exist and are not yet excluded by cosmological limits [1,2]. Indeed, the standard model of big bang nucleosynthesis (BBN) has difficulties in explaining the observed lithium production. The existence of a CMLLP that decays during or after the time of BBN could resolve this disagreement [3].

We derive cross-section limits for CMLLPs and compare them to theories of physics beyond the SM. In most supersymmetric (SUSY) models the lightest SUSY particle is assumed to be stable. Some SUSY models predict that the next-to-lightest supersymmetric particle (NLSP) can be a CMLLP. In this Letter we explore models that include a chargino as a NLSP. If its mass differs from the mass of the lightest neutralino by less than about 150 MeV, it can have a long lifetime [4,5]. This can occur in models with anomaly mediated supersymmetry breaking (AMSB) or in models that do not have gaugino mass unification. There are two general cases, where the chargino is mostly a Higgsino and where the chargino is mostly a gaugino, which we treat separately in this Letter.

There are some SUSY models that predict a long-lived scalar top quark (top squark) NLSP and a gravitino LSP. These top squarks hadronize into charged or neutral hadrons that are CMLLP candidates [6]. Hidden valley models predict scenarios where the top squark acts like the LSP and does not decay but also hadronizes into charged or neutral hadrons (referred to as R hadrons) that escape the detector [7,8]. In general, any SUSY scenario where the top squark is the lightest colored particle (which will happen in models without mass unification and heavy gluinos) can have a CMLLP. Any colored CMLLP will undergo hadronization and charge exchange during nuclear interactions, which we discuss below.

This search utilizes data collected between 2006 and 2010 with the D0 detector [9] at Fermilab's 1.96 TeV $p\bar{p}$ Tevatron Collider, and is based on 5.2 fb^{-1} of integrated luminosity. We reported previously [10] on a similar 1.1 fb^{-1} study, searching for events with a pair of CMLLPs, each with low speed. In addition to using the larger data sample, the present search looks for one or more CMLLP, rather than only for a pair, and characterizes CMLLPs with high dE/dx in addition to slow speed. Other searches for long-lived particles include those from the CDF Collaboration [11,12], the CERN e^+e^- Collider LEP [13], and the CERN pp Collider LHC [14,15].

The D0 detector [9] includes an inner tracker with two components: an innermost silicon microstrip tracker (SMT) and a scintillating fiber detector. We find a particle's dE/dx from the energy losses associated with its track in the SMT. The tracker is embedded within a 1.9 T superconducting solenoidal magnet. Outside the solenoid is a uranium or liquid-argon calorimeter surrounded by a muon spectrometer, consisting of drift-tube planes on either side of a 1.8 T iron toroid. There are three layers of the muon detector: the A layer, located between the calorimeter and the toroid, and the B and C layers, located outside the toroid. Each layer includes scintillation counters which serve to veto cosmic rays. Thus the muon system provides multiple time measurements from which a particle's speed may be calculated.

Because we distinguish CMLLPs solely by their speed β and dE/dx, we must measure these values for each muon candidate as accurately as possible. Muons from $Z \to \mu\mu$ events studied throughout the data sample allow calibration of the time measurement to better than 1 ns, with resolutions between 2–4 ns, and to maintain the mean dE/dx constant to within 2% over the data-taking period. From a specific muon scintillation counter we calculate a particle's speed from the time recorded and the counter's distance from the production point, and we compute an overall speed from the weighted average of these individual speeds, using measured resolutions. The ionization-loss data from the typically 8–10 individual energy deposits in the SMT are combined using an algorithm that corrects for track crossing angle and omits the largest deposit to reduce the effect of the Landau tail. We calibrate the dE/dx measurements by requiring that the dE/dx distribution of muons from $Z \to \mu\mu$ events has a maximum at 1. Figure 1 shows the distributions in β and dE/dx for data and background events that pass the selection criteria described below.

The selection of a candidate CMLLP occurs in several steps. Because of the high $p\bar{p}$ collision rate, we employ a three-level trigger system to reduce the event rate to the 200 Hz that can be recorded. The trigger system bases its decisions on characteristics of the event, which for the CMLLP candidates is the presence of a muon with a high momentum transverse to the beam direction (p_T). A time window at the initial trigger level reduces triggers on cosmic rays. This trigger gate lowers the trigger efficiency by 10% for CMLLPs with a mass of 300 GeV (as they will be slow and some will be out-of-time) and so contributes significantly to the overall acceptance. We avoid a tighter timing gate usually imposed at the second level of the muon trigger by accepting an alternative requirement that the muon have a matching track in the SMT.

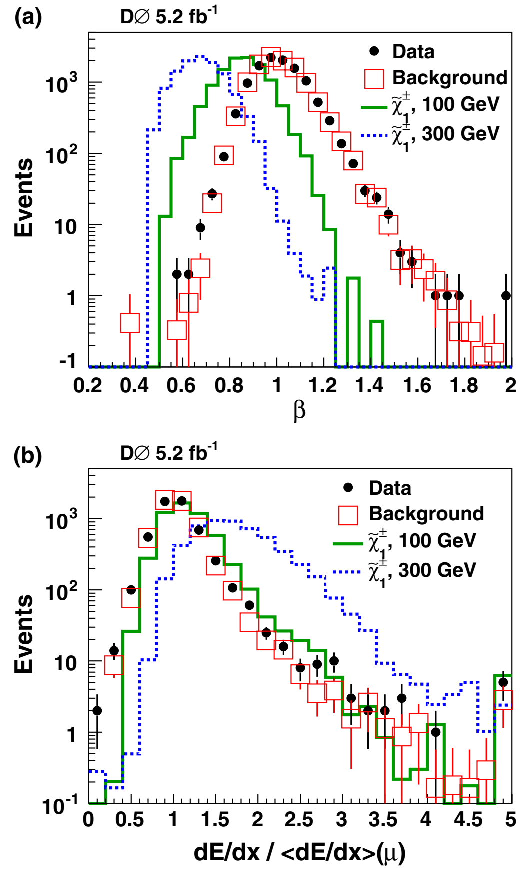

FIG. 1 (color online). Distributions of (a) speed β and (b) dE/dx for data, background, and signal (gauginolike charginos with a mass of 100 and 300 GeV) that pass the selection criteria. The histograms have been normalized to have the same numbers of events. We have adjusted the scale of the dE/dx measurements so that the dE/dx of muons from $Z \to \mu\mu$ events peak at 1. All entries exceeding the range of the histogram are added to the last bin.

In the standard D0 event reconstruction CMLLPs would appear as muons, which has been verified in detail using simulations. Thus, we select events with at least one well identified high p_T muon. For a reliable β measurement, the event must have scintillator hits in the A layer and either the B or C layer. We require at least three hits in the SMT, to obtain valid dE/dx data. For an optimal tracking and momentum measurement we require the muon to be central, i.e., with a pseudorapidity [16] $|\eta| < 1.6$. To reject muons from meson decays, we impose the isolation requirement that the sum of the p_T be less than 2.5 GeV for all other tracks in a cone of radius $R = \sqrt{(\Delta\phi)^2 + (\Delta\eta)^2} < 0.5$. We also require that the total transverse calorimeter energy in an annulus of radius $0.1 < R < 0.4$ about the muon direction be less than 2.5 GeV. A requirement that the z coordinate of the muon track at the location of closest approach to the beam axis be <40 cm ensures that the particle passes through the SMT.

We impose further criteria to eliminate cosmic rays. To select muons traveling outwards from the apparent interaction point, we require that its C-layer time be significantly greater than its A-layer time. We require also that the muon's distance-of-closest approach to the beam line be less than 0.02 cm. These criteria are also applied to additional muons in the event. For events with exactly two muons we require that the absolute value of the difference between each muon's A-layer times be less than 10 ns. To reject cosmic rays that appear as two back-to-back muons, we require that $\Delta\alpha = |\Delta\theta + \Delta\phi - 2\pi| > 0.05$.

Events with a muon from a W boson decay, with mismeasurements providing inaccurate values of the muon's β and dE/dx, constitute a potentially large background. To study rejection criteria for this background, we select data with transverse mass $M_T < 200$ GeV [17] to model the data in the absence of signal [18]. We choose selection criteria that minimize the number of events surviving from this background sample compared to events from simulations of the CMLLP signal. We require that events contain at least one muon with $p_T > 60$ GeV. From a separate sample of muons from $Z \to \mu\mu$ decays we observe that the association of a spurious scintillator hit with a muon track can result in an anomalously low β value. We use an algorithm that discards such hits through minimizing the χ^2/d.o.f. for the β calculated from the different scintillator layers. By comparing the effect on the background sample with the effect on simulated signal, we choose to eliminate events unless the minimized speed $\chi^2/\text{d.o.f.} < 2$. Finally, we compare the muon's track direction measured by the muon system with that measured in the central tracker, and eliminate events with clearly mismatched tracks.

To simulate signal events, we generate CMLLP candidates using PYTHIA [19], with specific models following those described in Ref. [20]. The long-lived top squarks are hadronized using [21]. Because the signature of the CMLLP cascade decays is model dependent and difficult to simulate accurately, we generate direct pair-production of the CMLLPs, without including cascade decays. We use the full D0 detector GEANT [22] simulation to determine the detector response for these samples (which include overlaid data-based $p\bar{p}$ interactions). The results are applicable to models with pair-produced CMLLPs with similar kinematics.

The top squarks form charged or neutral R hadrons, which may flip their charge as they pass through the detector. In the simulation, approximately 60% of R hadrons are charged following initial hadronization [23]; i.e., 84% of the events will have at least one charged R hadron. Further, R hadrons may flip their charge through nuclear interactions as they pass through material. We assume that R hadrons have a probability of 2/3 of being charged after multiple nuclear interactions and anti–R hadrons a probability of 1/2 of being charged, consistent with the numbers of possible hadronic final states [24–26]. For this analysis we require the R hadron to be charged before and after passing through the calorimeter, i.e., to be detected both in the tracker and in the A layer, and to be charged after the toroid, i.e., to be detected in the B or C layers. The probability for at least one of the R hadrons being detected is then 38%, or 84% if charge flipping does not occur. We include these numbers as normalization factors in the confidence-level analysis discussed below.

Our final selection criterion is that the candidate's speed $\beta < 1$. Thus, we describe the background by the $\beta < 1$ data events with $M_T < 200$ GeV, and search for CMLLP candidates in $\beta < 1$ data with $M_T > 200$ GeV. We normalize the background and data samples in the $\beta > 1$ region, where the contribution of signal is negligible. The uncertainties in the speed measurements depend on the particle's η, due to detector geometry. Since the distributions in η of the muons in the $M_T < 200$ GeV sample differ from those in the $M_T > 200$ GeV sample, we use the signal-free region to derive correction factors for the background sample that match its η distribution to that of the data.

We utilize a boosted decision tree (BDT) [27] to discriminate signal from background. The most discriminating variables are the CMLLP candidate's β and dE/dx, but we also include several related variables: the speed significance, defined as $(1 - \beta)/\sigma_\beta$, the corresponding number of scintillator hits, the energy loss significance defined as $(dE/dx - 1)/\sigma_{dE/dx}$, and the number of SMT hits. For each mass point in all three signal models we train the BDT with the signal simulation and the background, and then apply it to the data samples. Figure 1 shows the distributions in β and in dE/dx for the data and background samples, as well as for two representative signals.

Systematic uncertainties are studied by applying variations to the background and signal samples and determining the deviations in the BDT output distributions. Two of the systematic uncertainties affect the shape of the BDT distribution of signal and their effect is taken into account explicitly in the limit calculation: the uncertainty due to the width of the level 1 trigger gate and the uncertainty in the corrections to the simulation's time resolution. By examining the signal-like region of the BDT distributions, we find that the maximum (average) uncertainty is 10% (4%) for the trigger gate width, and 38% (7%) for the time resolution correction. All other systematic uncertainties affect only the normalization of the BDT output. The systematic uncertainties on the background are due to the dE/dx modeling ($< 0.1\%$) and the background normalization, from the specific values used for the β (7.2%) and M_T requirements (2.2%). The systematic uncertainties on the signal include muon identification (2%) and the integrated luminosity (6.1%) [28]. The systematic uncertainties associated with the corrections to the muon p_T resolution and to the dE/dx resolution, as well as the choice of parton distribution function and factorization scale, are all below 1%.

We obtain the 95% C.L. cross-section limits from the BDT output distributions, constraining systematic uncertainties to data in background dominated regions [29]. These limits are shown in Fig. 2, together with the next-to-leading order (NLO) theoretical signal cross sections, computed with PROSPINO [30]. Using the nominal (nominal -1 standard deviation) values of the NLO cross section, we are able to exclude gauginolike charginos below 267 (265) GeV and Higgsino-like charginos below 217 (214) GeV [31]. For top squarks, we assume a charge survival probability of 38%, as discussed above, and exclude masses below 285 (275) GeV. If charge flipping does not occur, we obtain a higher mass limit, as indicated in Fig. 2(c).

As shown in Fig. 2, the observed limit exceeds the expected limit at various mass points by as much as 2.5 standard deviations, for all signals tested, due to the presence of the same few data events with high BDT discriminant values. This discrepancy reflects the excess of data compared to background observed in Fig. 1 for the distributions both in β (around 0.6) and dE/dx (around 2.8). The kinematics of these events are consistent with a statistical fluctuation of the background.

In the mass range 200–300 GeV the observed cross-section limits shown in Fig. 2 are of the order 0.01 pb for both chargino signals and for the top squark signal with the charge survival factor removed. Since we consider only direct pair production and neglect the contribution of cascade decays, the signal cross sections and the kinematics mainly depend on the mass rather than on details of each individual model [32]. Thus, we are able to place a cross-section limit of order 0.01 pb, for directly produced CMLLPs in this mass range.

In summary, we perform a search for charged, massive long-lived particles using 5.2 fb^{-1} of integrated luminosity with the D0 detector. We find no evidence of signal and set 95% C.L. cross-section upper limits of order 0.01 pb for pair-produced CMLLPs of mass 200–300 GeV. At 95% C.L. we exclude pair-produced long-lived top squarks with mass below 285 GeV, gauginolike charginos below 267 GeV, and Higgsino-like charginos below 217 GeV. These are presently the most restrictive limits for chargino CMLLPs, with about a factor of 5 improvement over the previous D0 cross-section limits [10].

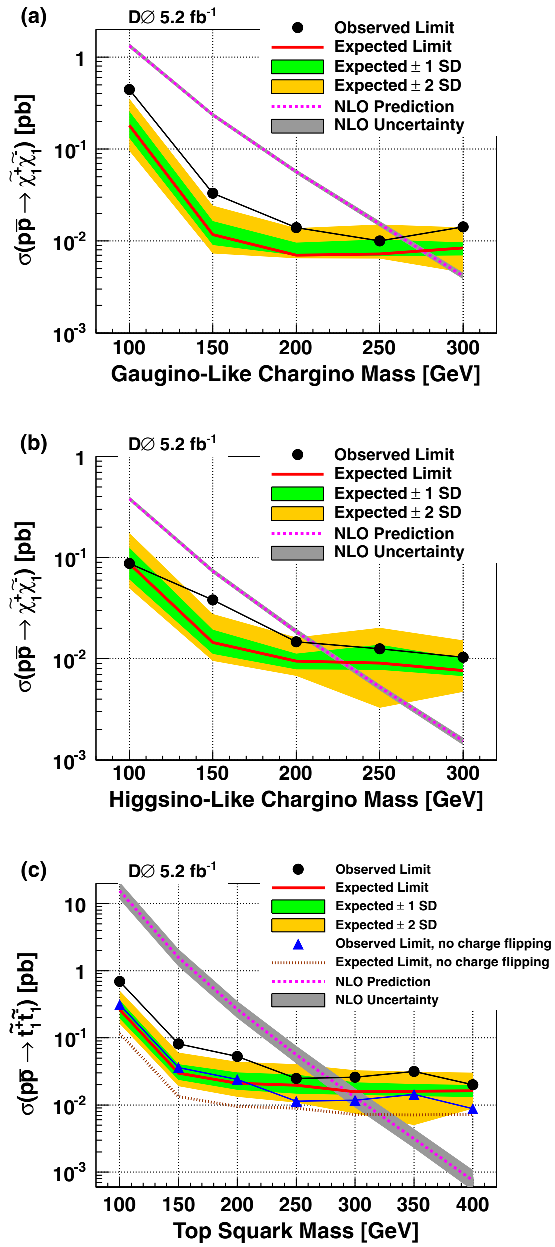

FIG. 2 (color online). Cross-section limits at 95% C.L. as a function of mass for (a) gauginolike charginos, (b) Higgsino-like charginos, and (c) top squarks. The top squark limits are displayed for the assumed charge flipping (charge survival probability = 38%) and for no charge flipping (charge survival probability = 84%).

We thank the staffs at Fermilab and collaborating institutions, and acknowledge support from the DOE and NSF (U.S.); CEA and CNRS/IN2P3 (France); FASI, Rosatom and RFBR (Russia); CNPq, FAPERJ, FAPESP, and FUNDUNESP (Brazil); DAE and DST (India); Colciencias (Colombia); CONACyT (Mexico); KRF and KOSEF (Korea); CONICET and UBACyT (Argentina); FOM (The Netherlands); STFC and the Royal Society (U.K.); MSMT and GACR (Czech Republic); CRC

Program and NSERC (Canada); BMBF and DFG (Germany); SFI (Ireland); The Swedish Research Council (Sweden); and CAS and CNSF (China).

*Deceased.
†Visitor from Augustana College, Sioux Falls, SD, USA.
‡Visitor from The University of Liverpool, Liverpool, U.K.
§Visitor from UPIITA-IPN, Mexico City, Mexico.
‖Visitor from SLAC, Menlo Park, CA, USA.
¶Visitor from University College London, London, U.K.
**Visitor from Centro de Investigacion en Computacion-IPN, Mexico City, Mexico.
††Visitor from ECFM, Universidad Autonoma de Sinaloa, Culiacán, Mexico.
‡‡Visitor from Universität Bern, Bern, Switzerland.

[1] M. Byrne, C. Kolda, and P. Regan, Phys. Rev. D **66**, 075007 (2002).
[2] K. Kohri *et al.*, Phys. Lett. B **682**, 337 (2010).
[3] K. Nakamura *et al.* (Particle Data Group), J. Phys. G **37**, 075021 (2010); see Big Bang Nucleosynthesis (rev.), Section 20.5, and references cited therein.
[4] J. F. Gunion and S. Mrenna, Phys. Rev. D **62**, 015002 (2000).
[5] C. H. Chen, M. Drees, and J. F. Gunion, Phys. Rev. D **55**, 330 (1997).
[6] G. F. Giudice and A. Rattazzi, Phys. Rep. **322**, 419 (1999).
[7] M. Strassler, arXiv:hep-ph/0607160.
[8] M. Strassler and K. Zurek, Phys. Lett. B **651**, 374 (2007).
[9] V. M. Abazov *et al.* (D0 Collaboration), Nucl. Instrum. Methods Phys. Res., Sect. A **565**, 463 (2006); M. Weber (D0 Collaboration), Nucl. Instrum. Methods Phys. Res., Sect. A **566**, 182 (2006); M. Abolins *et al.* (D0 Collaboration), Nucl. Instrum. Methods Phys. Res., Sect. A **584**, 75 (2008).
[10] V. M. Abazov *et al.* (D0 Collaboration), Phys. Rev. Lett. **102**, 161802 (2009).
[11] D. Acosta *et al.* (CDF Collaboration), Phys. Rev. Lett. **90**, 131801 (2003).
[12] T. Aaltonen *et al.* (CDF Collaboration), Phys. Rev. Lett. **103**, 021802 (2009).
[13] ALEPH, DELPHI, L3, and OPAL Collaborations, Report No. LEPSUSYWG/02-05.1; Report No. LEPSUSYWG/02-09.2.
[14] V. Khachatryan *et al.* (CMS Collaboration), J. High Energy Phys. 03 (2011) 024.
[15] G. Aad *et al.* (ATLAS Collaboration), Phys. Lett. B **698**, 353 (2011).
[16] The D0 coordinate system is cylindrical with the z axis along the proton beam direction, and the polar and azimuthal angles are denoted by θ and ϕ, respectively. The pseudorapidity is defined as $\eta = -\ln[\tan(\theta/2)]$.
[17] The transverse mass is defined by $M_T = \sqrt{(E_T + \not{E}_T)^2 - (p_x + \not{E}_x)^2 - (p_y + \not{E}_y)^2}$, where E_T is the total energy transverse to the axis of the colliding beams, and $\not{E}_T$ is the total unbalanced or missing transverse energy. The E_T and $\not{E}_T$ are measured using calorimeter deposits corrected for identified jets and leptons.
[18] The requirement $M_T < 200$ GeV is used to select W events. There is negligible contamination of potential signal events in this data sample.
[19] T. Sjöstrand, S. Mrenna, and P. Skands, J. High Energy Phys. 05 (2006) 026.
[20] P. Abreu *et al.* (DELPHI Collaboration), Eur. Phys. J. C **11**, 1 (1999). In the present analysis, for gauginolike charginos, $\mu = 10^4$ GeV, M_2 is approximately equal to the mass of the lightest chargino, and $M_1 = 3M_2$. For Higgsino-like chargino production, $M_1 = M_2 = 10^5$ GeV and μ is approximately equal to the mass of the lightest chargino. In the case of top squark production, the mass of the right-handed top squark is the mass given in the analysis; the mass of the left-handed top squark is 1.5 times heavier, and $\mu = 10^4$ GeV, $M_1 = 100$ GeV, and $M_2 = 200$ GeV. In all three models, $\tan\beta = 15$, $M_3 = 500$ GeV, and $M_{\mathrm{sq}} = 800$ GeV.
[21] The code for generating top squarks is at http://projects.hepforge.org/pythia6/examples/main78.f.
[22] R. Brun and F. Carminati, CERN Program Library Long Writeup W5013, 1993 (unpublished).
[23] M. Fairbairn *et al.*, Phys. Rep. **438**, 1 (2007).
[24] R. Mackeprang and A. Rizzi, Eur. Phys. J. C **50**, 353 (2007).
[25] R. Mackeprang and D. Milstead, Eur. Phys. J. C **66**, 493 (2010).
[26] R. Mackeprang, Report No. CERN-THESIS-2007-109.
[27] B. P. Roe *et al.*, Nucl. Instrum. Methods Phys. Res., Sect. A **543**, 577 (2005).
[28] T. Andeen *et al.*, Report No. FERMILAB-TM-2365, 2007.
[29] W. Fisher, FERMILAB Report No. TM-2386-E, 2007.
[30] W. Beenakker *et al.*, Phys. Rev. Lett. **83**, 3780 (1999).
[31] The two chargino scenarios have been excluded for masses below 100 GeV (Refs. [10,13]).
[32] Differences in production diagrams explain the different acceptances and thus somewhat different cross-section limits, for the two chargino scenarios.